

Oxygen removal from nitrogen using $\text{YBaCo}_2\text{O}_{5+\delta}$ adsorbent

Haoshan Hao^{***†}, Bojun Chen^{***}, Limin Zhao*, and Xing Hu**

*Department of Mathematical and Physical Sciences, Henan Institute of Engineering, Zhengzhou 451191, China

**Key Laboratory of Material Physics of Ministry of Education, Zhengzhou University, Zhengzhou 450052, China

***Department of Physics and Electronic Engineering, Zhoukou Normal University, Zhoukou 466001, China

(Received 27 January 2010 • accepted 10 June 2010)

Abstract—The oxygen intake/release behavior of $\text{YBaCo}_2\text{O}_{5+\delta}$ and its application as a medium-temperature (100–600 °C) adsorbent to oxygen removal in nitrogen purification was investigated. The oxygen content in $\text{YBaCo}_2\text{O}_{5+\delta}$ was varied between 5.46 and 5.0 with the change of the temperature and oxygen partial pressure. This oxygen nonstoichiometry showed good reversibility and the crystal structure of $\text{YBaCo}_2\text{O}_{5+\delta}$ remained stable in the oxygen intake/release process. Results of nitrogen purification experiment show that $\text{YBaCo}_2\text{O}_{5+\delta}$ material is a promising candidate to remove trace oxygen from nitrogen. After being deoxidized at 600 °C in nitrogen, 1 kg $\text{YBaCo}_2\text{O}_{5+\delta}$ adsorbent can purify 310 L nitrogen of 98.1% to high-purity nitrogen of over 99.9999% in one cycle.

Key words: $\text{YBaCo}_2\text{O}_{5+\delta}$, Oxygen Intake/Release, Adsorbent, Nitrogen Purification

INTRODUCTION

Oxygen content in many perovskite oxides is changeable with the temperature and surrounding oxygen partial pressure because of the variable valence state of transition metals. This oxygen nonstoichiometry makes it possible for oxygen ions to intake/release in these oxides, which has been utilized in fields such as solid-oxide fuel cells, gas separation, and catalysts [1,2]. Several perovskite-type oxides have been reported as high-temperature adsorbents for gas separation and purification [3–7]. These materials theoretically have an infinitely high selectivity for oxygen over nitrogen or other non-oxygen species.

The oxygen-deficient double perovskite structure compounds $\text{RBaCo}_2\text{O}_{5+\delta}$ (R represents rare-earth element) have attracted much attention during recent years because of their remarkable structural and electromagnetic properties. The crystal structure of these oxides can be regarded as a layered crystal $\text{A}'\text{A}''\text{B}_2\text{O}_6$ by doubling the unit cell of standard perovskite structure and consists of consecutive layers $[\text{CoO}_2]-[\text{BaO}]-[\text{CoO}_2]-[\text{RO}_\delta]$ stacked along the c axis [8,9]. The oxygen ions in the RO_δ layer can be easily varied in the range $0 \leq \delta \leq 1$ by means of heat treatment under appropriate atmosphere. The wide allowed range of oxygen content leads to several types of superstructure [8–17] and makes the $\text{RBaCo}_2\text{O}_{5+\delta}$ system a highly potential candidate for various applications such as oxygen storage and gas separation. Recently, Taskin et al. compared the oxygen diffusion behavior of the double perovskite structure $\text{GdBaMn}_2\text{O}_{5+\delta}$ and cubic perovskite structure $\text{Gd}_{0.5}\text{Ba}_{0.5}\text{MnO}_{5+\delta}$ [18]. They found that the oxygen-ion diffusion can be enhanced by orders of magnitude if a simple cubic phase transforms into a layered compound, which reduces the oxygen bonding strength and provides disorder-free channels for ion motion. Kim et al. also found that $\text{PrBaCo}_2\text{O}_{5+\delta}$ thin films have unusually rapid oxygen transport kinetics at low

temperature (300–500 °C), suggesting the potential application in the fields that require a fast oxygen transport such as a cathode material in solid oxide fuel cells [19]. In the present study, we investigated the oxygen intake/release behavior of $\text{YBaCo}_2\text{O}_{5+\delta}$ and its application prospect as adsorbent to remove oxygen from nitrogen.

EXPERIMENTAL PROCEDURES

1. Synthesis and Characterization of $\text{YBaCo}_2\text{O}_{5+\delta}$ Adsorbent

$\text{YBaCo}_2\text{O}_{5+\delta}$ adsorbent was prepared by the solid-state reaction method. The stoichiometric mixture of Y_2O_3 , BaCO_3 , and Co_3O_4 was milled with agate milling balls. After decarbonation at 1,000 °C, the powder was milled again and then rolled into balls of about 1.5-mm diameter using a sugar coater. The balls were sintered at 1,100 °C in air for 20 h and slowly cooled to room temperature. An iodometric titration method was used to measure the oxygen content of the sample. X-ray diffraction (XRD) analysis was carried out with X'pert Pro system using $\text{Cu K}\alpha$ radiation. Microstructure of $\text{YBaCo}_2\text{O}_{5+\delta}$ balls was observed by a scanning electron microscopy (SEM, Model JSM-5610LV, JEOL, Japan).

2. Measurement of Oxygen Intake/Release Properties

Thermogravimetry (TG) measurements were performed with a thermo-analyzer (SETARAM, Labsys™) to investigate the oxygen intake/release properties of $\text{YBaCo}_2\text{O}_{5+\delta}$ sample. About 100 mg $\text{YBaCo}_2\text{O}_{5+\delta}$ powder was examined in these experiments. A particle size analyzer (BT-3000A, Better, China) was used to analyze the grain size distribution and specific surface of the powders. The average grain size of the powder is $1.40 \mu\text{m}$ and the specific surfaces is $2.23 \times 10^4 \text{ cm}^{-2}$ in these experiments. In the first TG experiment, $\text{YBaCo}_2\text{O}_{5+\delta}$ powder was first heated from room temperature to 1,000 °C with the heating rate of 5 °C/min and then cooled to room temperature with same rate in air. In the second TG experiment, the powder sample was heated to 100 °C, 200 °C, 300 °C, 400 °C, 500 °C, 600 °C and 700 °C, respectively, and held at each temperature in oxygen (purity >99.99%) flow. When the mass of the sample did not change

[†]To whom correspondence should be addressed.
E-mail: hao@haue.edu.cn

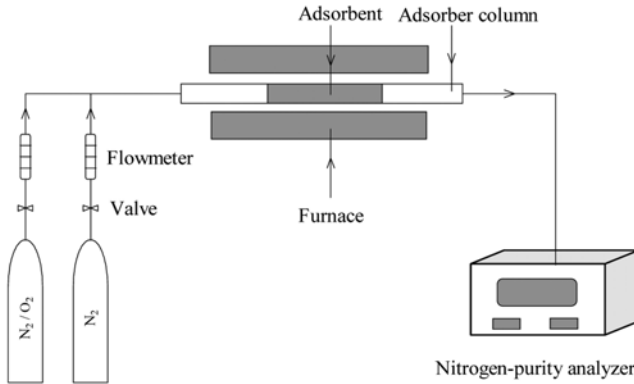


Fig. 1. The sketch of the experimental setup of oxygen removal from nitrogen.

any more, oxygen was quickly switched to nitrogen (purity >99.999%). Then nitrogen was changed to oxygen again when the mass did not decrease markedly. The flow of the nitrogen and oxygen was 30 mL/min.

3. Experiments of Oxygen Removal in Nitrogen

The experimental setup of oxygen removal from nitrogen includes a gas delivery system, an adsorber column, a tubular furnace, and a nitrogen-purity analyzer (model DFY-4, Taige, China). The experimental setup is shown in Fig. 1. The column is made from a stainless steel tube of 3.1-cm inner diameter. 1.0 kg $\text{YBaCo}_2\text{O}_{5+\delta}$ balls were packed in the column and the length of the adsorbent is about 40 cm. The column was put into a tubular furnace. Nitrogen-oxygen mixture with the oxygen concentration of 1.9% was used as the feed gas for purification. The flow of the feed gas was maintained at 300 mL/min. The nitrogen concentration in the effluent of the column was continuously monitored by a nitrogen-purity analyzer. The analyzer uses a zirconia oxygen sensor to detect oxygen concentration ($\text{O}_2\%$) in nitrogen. Nitrogen concentration ($\text{N}_2\%$) is given according to $\text{N}_2\% = 1 - \text{O}_2\%$. The device can measure oxygen concentration from percentage levels to less than 1 ppm with autoranging. The adsorbent was first heated to 600 °C, held at this temperature for 10 min, and then cooled to work temperature in nitrogen. The work temperatures were kept at a constant point during the adsorption processes and limited in the range of 100–600 °C. The oxygen adsorption capacity was calculated by the oxygen concentration, the feed gas flow, and the adsorption time, where the adsorption time was recorded with the purity of effluent nitrogen over 99.9999%. When the nitrogen purity was smaller than 99.9999%, the adsorbent was heated to 600 °C in nitrogen to regeneration.

RESULTS AND DISCUSSION

Iodometric titration results show that the oxygen content in the air-synthesized samples is 5.46. When the sample was heat-treated at 600 °C in nitrogen, the oxygen content was reduced to 5.03. Fig. 2 shows the XRD patterns of the air-synthesized $\text{YBaCo}_2\text{O}_{5+\delta}$ powder sample and the sample after heat treatment at 600 °C in nitrogen. The crystal structure of the air-synthesized sample can be indexed with double perovskite structure with tetragonal $3a_p \times 3a_p \times 2a_p$ supercells (a_p being the cell parameter of cubic perovskite). A tripling of a and b parameter results from the ordering of oxygen va-

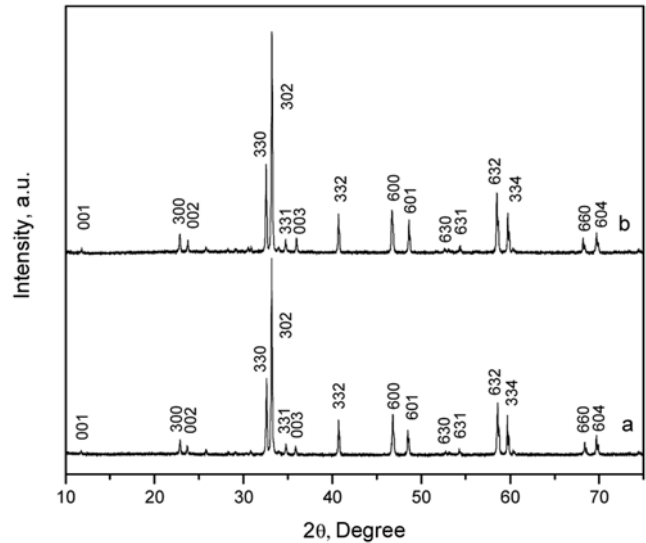


Fig. 2. X-ray diffraction patterns of $\text{YBaCo}_2\text{O}_{5+\delta}$, (a) air-prepared sample ($\delta=0.46$) and (b) the heat-treated sample ($\delta=0.03$).

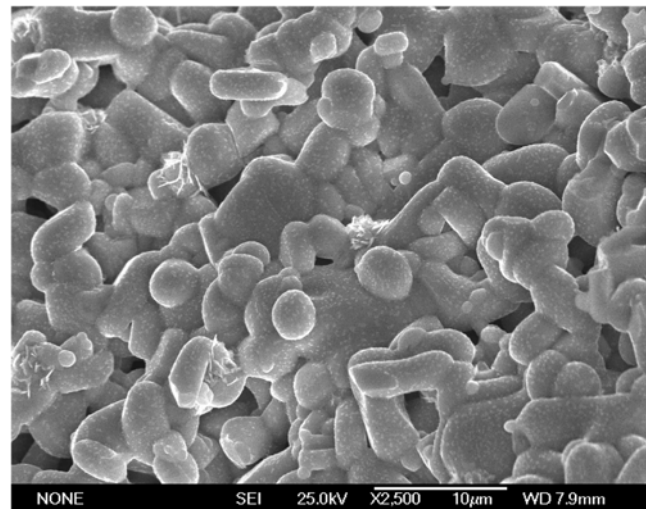


Fig. 3. SEM photograph of $\text{YBaCo}_2\text{O}_{5+\delta}$ ball.

cancies in the YO_δ layer [9]. The XRD pattern of the heat-treated sample is similar to that of the air-synthesized sample, suggesting strong structural stability of $\text{YBaCo}_2\text{O}_{5+\delta}$.

Fig. 3 shows the microstructure of $\text{YBaCo}_2\text{O}_{5+\delta}$ balls. The grain sizes are several microns and the ball is not dense due to the non-pressure molding. The appearance of pores will provide the channels favoring the oxygen intake and release.

Fig. 4 shows the mass change of $\text{YBaCo}_2\text{O}_{5.46}$ with temperature in air. TG curve shows that the mass of the sample is almost unchanged in the range of RT–300 °C. When the temperature is above about 300 °C, however, the sample begins to release oxygen and the mass decreases with the increase of temperature. The mass loss is about 1.7% of its original mass when temperature reaches 1,000 °C, corresponding to 0.458 oxygen ions released from a unit cell of $\text{YBaCo}_2\text{O}_{5.46}$. When temperature decreases to room temperature, the released oxygen can be completely absorbed into the sample again. The second-cycle experiment shows that this oxygen release and

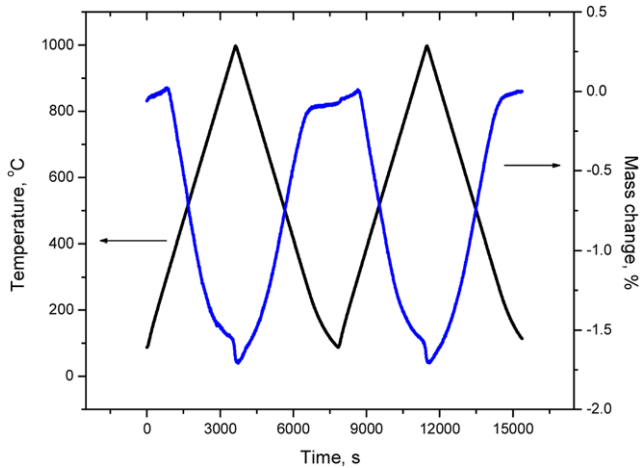


Fig. 4. Mass change of $\text{YBaCo}_2\text{O}_{5+\delta}$ with temperature in air.

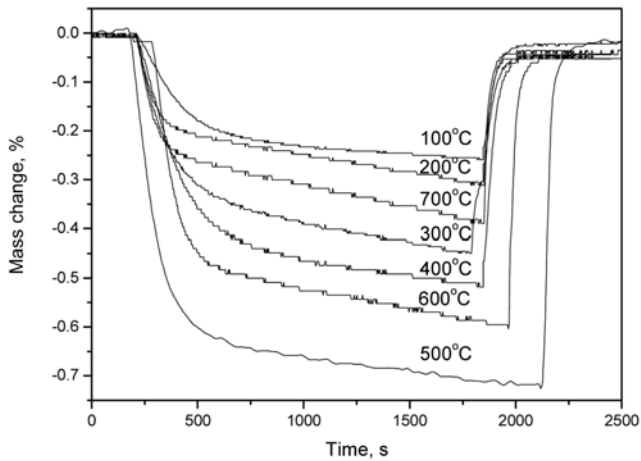


Fig. 5. Mass change of $\text{YBaCo}_2\text{O}_{5+\delta}$ during $\text{O}_2 \rightarrow \text{N}_2 \rightarrow \text{O}_2$ cycle at different temperature.

intake process has a good reproducibility.

Fig. 5 shows the mass change of $\text{YBaCo}_2\text{O}_{5+\delta}$ sample as the gas flow is switched between oxygen and nitrogen at 100–700 °C. Like other perovskite oxides [20–22], oxygen content in $\text{YBaCo}_2\text{O}_{5+\delta}$ is also tunable when the surrounding oxygen partial pressure is changed. A common feature of these figures is that the mass will decrease (release oxygen) when gas flow is changed from oxygen to nitrogen and increase (absorb oxygen) when gas flow is changed from nitrogen to oxygen at each temperature.

Using the transient thermogravimetric data in Fig. 5, one can obtain oxygen adsorption/desorption rate constants k_a and k_d based on the theoretical model proposed by Zeng et al. [20]. In the model, the following equation is used to calculate the lumped surface reaction constants k_a and k_d :

$$\ln \left[\frac{w(t) - w(e)}{w(0) - w(e)} \right] = -2\phi kt \quad (1)$$

In this equation, $w(0)$ is weight of the powder at the time of gas flow switching (scale as $t=0$), $w(e)$ is the steady state weight of the sample after the gas flow change, and ϕ is the specific area of the powder. When the atmosphere is switched from nitrogen to oxy-

Table 1. Oxygen adsorption rate constants and desorption rate constants of $\text{YBaCo}_2\text{O}_{5+\delta}$ powder

T (°C)	100	200	300	400	500	600	700
$k_a (10^{-7} \text{ cm} \cdot \text{s}^{-1})$	3.45	3.93	4.16	4.65	8.76	8.43	5.94
$k_d (10^{-7} \text{ cm} \cdot \text{s}^{-1})$	0.78	0.86	0.93	1.09	1.93	2.54	2.13

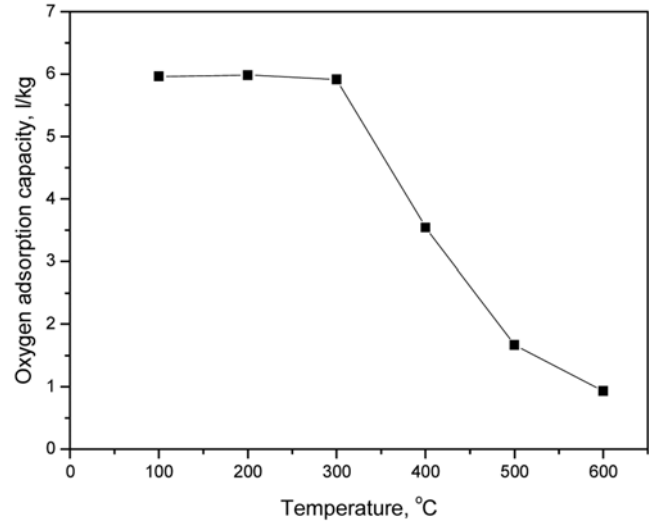


Fig. 6. Oxygen adsorption capacity of $\text{YBaCo}_2\text{O}_{5+\delta}$ adsorbent at different temperature.

gen, k is oxygen adsorption rate constant k_a , and when the atmosphere is switched from oxygen to nitrogen, k is oxygen desorption rate constant k_d . Plotting $\ln[(w(t)-w(e))/(w(0)-w(e))]$ versus time t , one can obtain the slope $-2\phi k$ and then k_a and k_d .

The calculated oxygen adsorption/desorption rate constants k_a and k_d of $\text{YBaCo}_2\text{O}_{5+\delta}$ are presented in Table 1. The values are larger than those of cubic perovskite oxides [22], suggesting the potential application in the fields that require a fast oxygen transport.

As a conclusion from the results shown in Figs. 4 and 5, the oxygen content in $\text{YBaCo}_2\text{O}_{5+\delta}$ can be changed with the temperature and oxygen partial pressure. Oxygen intake at low temperature or at high oxygen partial pressure, oxygen release at high temperature or at low oxygen partial pressure, fast oxygen adsorption/desorption kinetics, and the reversibility of this oxygen intake/release process make $\text{YBaCo}_2\text{O}_{5+\delta}$ a potential candidate as adsorbent to realize gas separation or purification.

Oxygen removal experiments show that when the sample was heat-treated at 600 °C in nitrogen, the purity of effluent nitrogen can exceed 99.999% when operated at the temperatures varying from 100 °C to 600 °C. Fig. 6 shows the oxygen adsorption capacity of $\text{YBaCo}_2\text{O}_{5+\delta}$ adsorbent at different temperatures. It can be seen that oxygen adsorption capacity is about 6.0 L/kg in the range of 100–300 °C. In other words, 1 kg $\text{YBaCo}_2\text{O}_{5+\delta}$ adsorbent can purify 310 L nitrogen of 98.1% to high-purity nitrogen of over 99.9999% in one cycle. With the increase of the work temperature, the oxygen adsorption capacity will rapidly decrease due to the decrease of equilibrium oxygen content in $\text{YBaCo}_2\text{O}_{5+\delta}$. This change of oxygen adsorption capacity with the temperature is consistent with the transient TG result shown in Fig. 4. In the oxygen removal experiments,

the calculated equilibrium oxygen content in $\text{YBaCo}_2\text{O}_{5+\delta}$ is about 5.23 in the range of 100–300 °C. As shown in Fig. 4, however, the oxygen content in the same temperature range is about 5.46 in air. The reason is that oxygen partial pressure of the feed gas in the oxygen removal experiments is lower than that in air, which results in the decrease of equilibrium oxygen content in the oxygen removal experiments.

CONCLUSIONS

The oxygen intake/release behavior of $\text{YBaCo}_2\text{O}_{5+\delta}$ and its application to oxygen removal from nitrogen was investigated. The oxygen content in $\text{YBaCo}_2\text{O}_{5+\delta}$ is reduced from 5.46 to about 5.0 by increasing the temperature to 1,000 °C or by heat-treating at 600 °C in nitrogen. The crystal structure of $\text{YBaCo}_2\text{O}_{5+\delta}$ is stable with the oxygen nonstoichiometry. Results of nitrogen purification experiment show that this material can be used as medium-temperature adsorbent to produce high-purity nitrogen. After being deoxidized at 600 °C in nitrogen, 1kg $\text{YBaCo}_2\text{O}_{5+\delta}$ adsorbent can purify 310 L nitrogen of 98.1% to high-purity nitrogen of over 99.9999% in one cycle.

ACKNOWLEDGEMENTS

This research was supported by the Science and Technology Foundation of Henan Province, China (No. 092102210263) and the Program for Innovative Research Team (in Science and Technology) in Henan Institute of Engineering (No. 2009IRTHNIE05).

REFERENCES

- M. Hunsom, L. A. Dunyushkina and S. B. Adler, *Korean J. Chem. Eng.*, **23**, 720 (2006).
- J. H. Park and S. D. Park, *Korean J. Chem. Eng.*, **24**, 897 (2007).
- S. Guntuka, S. Farooq and A. Rajendran, *Ind. Eng. Chem. Res.*, **47**(1), 163 (2008).
- Q. H. Yin, J. Kniep and Y. S. Lin, *Chem. Eng. Sci.*, **63**, 2211 (2008).
- Z. H. Yang, Y. S. Lin and Y. Zeng, *Ind. Eng. Chem. Res.*, **41**, 2775 (2002).
- D. L. Yang, J. Mo, H. X. Lu, Y. Q. Guo, Z. S. Gao and X. Hu, *J. Rare Earths*, **23**, 112 (2005).
- Z. H. Yang and Y. S. Lin, *Ind. Eng. Chem. Res.*, **42**, 4376 (2003).
- A. Maignan, C. Martin, D. Pelloquin, N. Nguyen and B. Raveau, *J. Solid State Chem.*, **142**, 247 (1999).
- D. Akahoshi and Y. Ueda, *J. Solid State Chem.*, **156**, 355 (2001).
- C. Frontera, A. Caneiro, A. E. Carrillo, J. Oro-Sole and J. L. Garcia-Munoz, *Chem. Mater.*, **17**, 5439 (2005).
- E. Suard, F. Fauth and V. Caignaert, *Physica B*, **276-278**, 254 (2000).
- T. Vogt, P. M. Woodward, P. Karen, B. A. Hunter, P. Henning and A. R. Moodenbaugh, *Phys. Rev. Lett.*, **84**, 2969 (2000).
- E. Suard, F. Fauth, V. Caignaert, I. Mirebeau and G. Baldinozzi, *Phys. Rev. B*, **61**, 11871 (2000).
- I. O. Troyanchuk, N. V. Kasper, D. D. Khalyavin, H. Szymczak, R. Szymczak and M. Baran, *Phys. Rev. Lett.*, **80**, 3380 (1998).
- Y. Moritomo, T. Akimoto, M. Takeo, A. Machida, E. Nishibori, M. Takata, M. Sakata, K. Ohoyama and A. Nakamura, *Phys. Rev. B*, **61**, 13325 (2000).
- A. A. Taskin, A. N. Lavrov and Y. Ando, *Phys. Rev. B*, **73**, 121101 (2006).
- C. Martin, A. Maignan, D. Pelloquin, N. Nguyen and B. Raveau, *Appl. Phys. Lett.*, **71**, 1421 (1997).
- A. A. Taskin, A. N. Lavrov and Y. Ando, *Appl. Phys. Lett.*, **86**, 091910 (2005).
- G. Kim, S. Wang, A. J. Jacobson, Z. Yuan, W. Donner, C. L. Chen, L. Reimus, P. Brodersen and C. A. Mims, *Appl. Phys. Lett.*, **88**, 024103 (2006).
- Y. Zeng and Y. S. Lin, *Solid State Ionics*, **110**, 209 (1998).
- J. Hu, X. Hu, H. S. Hao, L. J. Guo, H. Z. Song and D. L. Yang, *Solid State Ionics*, **176**, 487 (2005).
- J. Hu, H. S. Hao, C. P. Chen, D. L. Yang and X. Hu, *J. Membr. Sci.*, **280**, 809 (2006).